THE LARGE-SCALE MOTIONS IN NEUTRAL AND STABLY STRATIFIED WALL-TURBULENCE

Makoto Tsubokura*and Tetsuro Tamura
Department of Environmental Science and Technology,
Tokyo Institute of Technology
Nagatsuta 4259, Midori-ku, Yokohama 226-8502, Japan
tsubo@depe.titech.ac.jp, tamura@depe.titech.ac.jp

ABSTRACT

The large-scale structures observed at or above the logarithmic-layer of wall-turbulence were investigated using Large Eddy Simulation. We have mainly focused on the Reynolds-number scaling of the large-scales and the influence of thermal stratification on these motions. The grid resolution required for the reproduction of the large-scale structures in plane channels was intensively studied and it was found that rather higher grid resolution that was sufficient to reproduce the near-wall structures was required to properly reproduce the large-scale motions. This fact indicates that there would be a strong relation between the small-scales near the wall and the large-scales in the outer-layer. The large-scales in the neutral state basically obey the outer-scaling and their spanwise size was about twice larger than the boundary-layer thickness independent of the Reynolds number tested here. The large-scales were also found to be strongly affected by the thermal stratification and were suppressed at a certain weakly stable stratification tested here, contrarily to the fine-scale structures being rather insensitive to the thermal stratification.

INTRODUCTION

It has been widely acknowledged that there exist the large-scale structures in wall-turbulence with the size at least comparable to the boundary layer thickness. In contrast to the small-scale structures near the wall, less attention has been paid to the large scales until recently. Del Álamo & Jiménez(2001) argued that one of the reason for this relative neglect went back to Townsend's first prediction of the large-scales under the *attached eddy* hypothesis, in which he described them as *inactive* in the sense that they do not contain Reynolds stress. However recently, Jiménez(1998) showed from various existing experimental and numerical data that they were rather *active* containing substantial Reynolds stress as well as turbulence energy, which was later ensured by Direct Numerical Simulation (DNS) conducted by themselves. Furthermore Hunt and Morrison(2000) recently proposed the *top-down* structures of wall-turbulence, in which outer-layer structures affect the near-wall small scales a lot at very high Reynolds numbers such as observed in atmospheric boundary layer. In fact, the Reynolds number dependence of the streamwise velocity fluctuation near the wall (e.g., DeGraaff, 2000) seems to be explained as the result of the interaction between the small scales in the inner-layer and the large scales in the outer-layer.

*Present address: The University of Electro-Communications, Department of Mechanical Engineering and Intelligent Systems, Chofugaoka 1-5-1, Chofu-shi, Tokyo, 182-8585, Japan; tsubo@mce.uec.ac.jp.

On the other hand, increasing attention has been paid to the development of the artificial wall boundary condition for Large Eddy Simulation(LES) as one of the practical problems of turbulence simulation. In this context, the preceding fundamental argument for the large scales is essential to properly model the near wall turbulence. Therefore studying the large scales in the context of such as their origin, interactions with the near-wall structures, or Reynolds-number scaling is important to understand the structure of the high Reynolds number wall-turbulence from both fundamental and practical points of view.

The existence of the large scales has been recognised mainly by the experimental results of the abnormal extent of the temporal auto correlation of the streamwise velocity or the peak of the corresponding pre-multiplied one-dimensional power spectra at the low wavenumber region. In addition, Kim and Adrian(1999) recently pointed out from their measurements of fully developed turbulent pipe flow the existence of another large scale motions which are much larger than the ones comparable to the boundary layer thickness. They called them as *very* large scale motions. From these experimental results, we can suppose the large scale structures as the streamwise elongated anisotropic motions similar to the near wall streaks but of the size some times or even more larger than the boundary layer thickness. However in experimental studies, one-point measurements as one of the most popular methods has fundamental difficulty of capturing the spanwise structures. The validity of the spectrum converted from frequency to wavenumber using Taylor's hypothesis for the use of the large-scale analysis also should be considered carefully.

In addition, the practical difficulty of studying the large-scale structures lies in the fact that they require the large experimental setup or the computational domain at sufficiently large Reynolds number to properly capture their entire structures. This requirement has been the stumbling block for both experiments and DNS to investigate the large scales(e.g. Kawamura and Abe, 2002). In this context, LES seems to be the promising method, in which only the large and coherent flow structures are directly solved by the three-dimensional time-marching numerical simulation while rather isotropic and universal eddies are only modelled.

The purposes of this study are: firstly to examine intensively the grid resolution of LES required to reproduce the large-scales in fully developed incompressible turbulent plane channels; secondly to investigate the Reynolds number similarity of the large scales; finally to see how the stable stratification affects the large-scales.

Requirement of the excessively fine resolution, which is sufficient to reproduce the near-wall small eddies, obtained in the first part of this study unexpectedly reveals that small

scales near the wall play an important role on the process of producing the large scales in the outer-layer.

NUMERICAL METHODS

Analysis Models

We have adopted a simple open channel flow, in which no-slip and free-slip conditions are imposed on the lower and upper walls respectively, as one of the typical wall-bounded turbulence. Hereafter streamwise, normal-wall and spanwise directions are given as x, y and z respectively. The flow field is considered to be periodic for streamwise and spanwise directions, and is driven by the uniform pressure gradient force acting for the streamwise direction to obtain the fully developed turbulence state. A constant heat flux is considered on both lower and upper walls with different values between them. Supposing that gravity acts for the negative y direction, zero- and negative-flux conditions on the upper and lower walls respectively are imposed to obtain the stably stratified state. To compensate the heat loss on the lower wall, fluid considered here is supposed to have an uniform heat source in the whole flow field, which is similar to the uniform pressure gradient in the velocity condition mentioned above(*see* the similarity of eqs.(2) and (3) shown below).

These boundary conditions for the velocity and temperature produce following two important numerical parameters to be determined *a priori*. One is the Reynolds number, $Re = u_\tau \delta/\nu$, and the other is the Richardson number, $Ri_\tau = \beta g Q \delta / u_\tau^3$, in which u_τ, ν, δ,β, g and Q are the friction velocity at the lower wall, the kinetic viscosity, channel-width, the volumetric expansion coefficient, gravitational acceleration and the heat flux on the lower wall respectively.

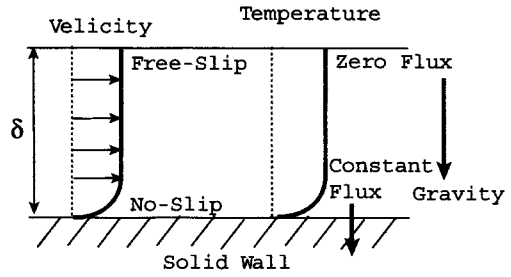

Figure 1: Analysis Model.

Governing Equations

We suppose fluid is incompressible and Newtonian, and a buoyancy term is modelled by the Boussinesq approximation. The governing equations of LES adopted in this study is obtained by spatially filtering the corresponding continuity, momentum and heat transfer equations:

$$\frac{\partial \bar{u}_i}{\partial x_i} = 0, \tag{1}$$

$$\frac{\partial \bar{u}_i}{\partial t} + \frac{\partial \bar{u}_i \bar{u}_j}{\partial x_j} = -\frac{\partial \bar{p}}{\partial x_i} + \frac{1}{Re_\tau}\frac{\partial^2 \bar{u}_i}{\partial x_j \partial x_j} - \frac{\partial}{\partial x_j}\tau_{ij} + Ri_\tau \bar{\theta}\delta_{i2} + \delta_{i1}, \tag{2}$$

$$\frac{\partial \bar{\theta}}{\partial t} + \frac{\partial \bar{\theta}\bar{u}_j}{\partial x_j} = \frac{1}{Re_\tau Pr}\frac{\partial^2 \bar{\theta}}{\partial x_j \partial x_j} - \frac{\partial}{\partial x_j} q_j + 1, \tag{3}$$

where Pr is the molecular Prandtl number, which is set to be 0.7 in this work. Here *overbar* denotes the *grid* filtering operation. The *subgrid*-scale (SGS) stress in (2) and the SGS heat flux in (3) must be modelled which is given as

$$\tau_{ij} = \overline{\bar{u}_i \bar{u}_j} - \bar{u}_i \bar{u}_j, \tag{4}$$

$$q_j = \overline{\bar{\theta} \bar{u}_j} - \bar{\theta}\bar{u}_j. \tag{5}$$

Subgrid-Scale modelling

In this study SGS stress and heat flux terms are modelled under the isotropic eddy viscosity assumption:

$$\tau_{ij} - \frac{1}{3}\delta_{ij}\tau_{kk} = -2C\frac{k}{3|\bar{S}|}\bar{S}_{ij}, \tag{6}$$

$$q_j = -C_\theta \frac{k}{3|\bar{S}|}\frac{\partial \bar{\theta}}{\partial x_j}, \tag{7}$$

where $\bar{S}$ is a magnitude of the strain rate tensor, $\bar{S}_{ij} = (\partial \bar{u}_i/\partial x_j + \partial \bar{u}_j/\partial x_i)/2$, and is given as $\bar{S} = \sqrt{2\bar{S}_{ij}\bar{S}_{ij}}$. We would like to note that these forms are different from the famous Smagorinsky's model, and that the SGS turbulence energy, k, is explicitly included in the eddy viscosity or diffusion coefficients. The model coefficients, C and C_θ, included in (6) and (7) are determined following the dynamic procedure(Germano et al., 1991 and Lilly, 1992). In the dynamic procedure, so-called *subtest*-scale (STS) stress,$T_{ij} = \widetilde{\bar{u}_i \bar{u}_j} - \tilde{\bar{u}}_i \tilde{\bar{u}}_j$, and corresponding heat flux also must be modelled. We would like to note that *overtilde* denotes the *test* filtering operation required in the dynamic procedure. Here the STS stress is modelled on the analogy of the SGS model given in (6) as follows,

$$T_{ij} - \frac{1}{3}\delta_{ij}T_{kk} = -2C\frac{K}{3|\tilde{\bar{S}}|}\tilde{\bar{S}}_{ij}, \tag{8}$$

where K is the STS turbulence energy. The SGS and STS energy in (6) and (8) are modelled considering the consistency of the numerical (finite difference) error in the dynamic procedure:

$$k = \overline{\bar{u}_k \bar{u}_k} - \bar{\bar{u}}_k \bar{\bar{u}}_k, \tag{9}$$

$$K = \widetilde{\bar{u}_k \bar{u}_k} - \tilde{\bar{\bar{u}}}_k \tilde{\bar{\bar{u}}}_k. \tag{10}$$

The notable features of these SGS models are; because of the consistency of the numerical error in the dynamic procedure, this model shows less sensitivity to the discrete *test* filtering operation than the usual dynamic procedure using the Smagorinsky's model. For the detail of the derivation of these models and their fundamental property in LES, refer to Tsubokura et al.(2001a) and Tsubokura(2001b).

Discretization

Governing equations are discretized on the staggered grid system based on the fully conservative finite difference scheme developed recently by Morinishi et al.(1998). The fourth-order accuracy is considered for all spatial derivatives except for the SGS terms. It should be noted here that the fourth order accuracy is determined from a compromise between the higher order requirement for SGS stress not to be dominated by numerical errors and the lower-order requirement for non-liner term not to be contaminated by the aliasing error (e.g., Ghosal, 1996). The third-order Runge-Kutta method is basically adopted as the time marching method, and the second derivative for the normal-wall direction included in the viscous term is only treated semi-implicitly using the Crank-Nicolson method for the tolerance

Table 1: Reynolds number in the neutral cases of the open channel flows.

$Re_\tau = u_\tau \delta/\nu$	395	590	1180
$Re_\delta = U_C \delta/\nu$	8.1×10^3	1.3×10^4	2.7×10^4

Table 2: Reynolds and Richardson numbers in the stable cases of the open channel flows.

$Re_\tau = u_\tau \delta/\nu$	1180			
$Ri_\tau = \beta g Q \delta/u_\tau^3$	0.45	0.9	2.7	4.5
$Re_\delta = u_C \delta/\nu (\times 10^4)$	3.0	3.2	4.1	4.9
$Ri_\delta = \beta g \Delta T \delta/u_C^2 (\times 10^{-2})$	1.35	2.56	6.00	8.42

of time increment in the numerical simulation. MAC method is used for the velocity-pressure coupling and the corresponding pressure Poisson equation is solved by the discrete FFT method for the periodic direction while the septa-diagonal method is adopted for the normal-wall direction.

Analysis Conditions

Neutral cases. Wall turbulence in neutral stratification is studied mainly to investigate the Reynolds-number scaling of the large-scale motions. Therefore LES at three different Reynolds numbers ranging from lower to moderate cases was conducted here. The Reynolds numbers defined by the friction velocity as an input parameter and their corresponding bulk Reynolds numbers are summarised in Table 1.

Stable cases. In the stably stratified wall-turbulence, three Richardson numbers,Ri_τ, are tested here while the Reynolds number, Re_τ, is fixed to 1180. It should be noted that due to the effect of the thermal stratification, the flow at the different Ri_τ of the same Re_τ produces the different bulk Reynolds number,$Re_\delta = u_C \delta/\nu$, where u_C is the bulk velocity. The Re_τ and Ri_τ as input numerical parameters and their corresponding Re_δ and the bulk Richardson number $Ri_\delta = \beta g \Delta T \delta/u_C^2$ are summarised in Table 2. In all stable conditions tested here, obtained bulk Richardson numbers are less than 0.1 and they are categorised as the weak stratification, in which turbulence is maintained in the whole flow field.

Domain sizes and grid numbers. The domain size and the grid number are the important parameters to study the large-scales. Because we have adopted the periodic conditions for both streamwise and spanwise directions, the largest scales captured by LES are restricted to half of the domain size, which should be ideally larger than the large-scales appearing in the real wall-turbulence.

As regards the latter one, LES permits us to determine the minimum scale of the directly resolved turbulence motion in our hands by considering the grid resolution, in contrast to the DNS in which even the Kolmogorov scale must be resolved as the smallest scales. This fact, in the other way rounds, requires us to investigate in detail as to whether the adopted numerical methods in LES properly resolve the objective motion. In this context, in addition to the open channel flow, the ordinary closed or confined plane channel flow, in which reliable DNS at the moderate Reynolds number has already been conducted, is also investigated intensively to determine the grid resolution required for the reproduction of large-scales.

The domain sizes and grid numbers adopted in this study are shown in Table 3. We can see that unexpectedly fine grids of $h_x^+ \sim 30$ and $h_z^+ \sim 20$ are finally adopted in this study. The determination of the grid resolution as well as the region sizes for the large-scales will be mentioned in the next section.

DEPENDENCE ON GRID RESOLUTIONS

Considering the fact that the spatial scales of the large-scales in the outer layer is at least comparable to the boundary layer thickness, it is expected that relatively coarse grids are sufficient to reproduce the large scales. On the other hand, if the large scale motion results from the small scales in the vicinity of the wall such as proposed in the Townsend's attached eddy hypothesis, required grids for large-scales will be unexpectedly fine to reproduce the near-wall turbulence. Accordingly in this section, we will try to find the proper grid resolution required for the large scale structures in LES from the physical as well as the practical point of view.

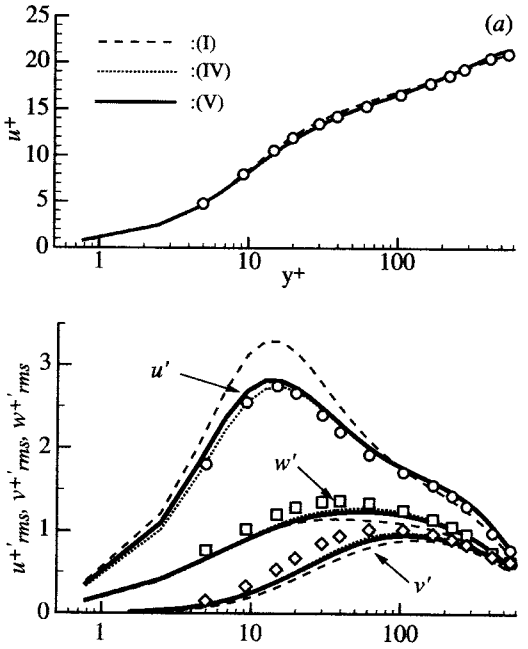

Figure 2: Turbulence statistics at $Re_\tau = 550$ (DNS) and 590(LES): symbol, DNS; line, LES; (a),mean velocity; (b), RMS of velocity fluctuation.

The moderate Reynolds number of 590 is adopted here in which reliable DNS data has been provided by del Álamo & Jiménez(2003). This DNS is known as the first simulation using the domain size large enough to study the large scales. It is acknowledged that the large-scales in the outer layer are described as the large elongated anisotropic structures with substantial energy only in the streamwise velocity component. In this respect, reproduction of the pre-multiplied one-dimensional power spectra of the streamwise velocity is investigated at various grid resolutions. Special attention is focused on the lower wavenumber region of the spectra in

Table 3: Numerical conditions of the open channel for the scaling

Re_τ	Ri_τ	*Domain size* $L_x \times L_y \times Lz$	*Grid number* $N_x \times N_y \times N_z$	*Grid spacing* h_x^+	h_z^+
395	0	$12\pi\delta \times \delta \times 2.25\pi\delta$	$576 \times 32 \times 144$	25.9	19.4
590	0		$768 \times 48 \times 216$		
1180	0/0.45		$1536 \times 64 \times 432$		
1180	0.9	$4\pi\delta \times \delta \times 2\pi\delta$	$512 \times 64 \times 384$	29.0	19.3
	2.7	$2\pi\delta \times \delta \times \pi\delta$	$256 \times 64 \times 192$		
	4.5	$2\pi\delta \times \delta \times \pi\delta$	$156 \times 64 \times 192$		

Table 4: Numerical conditions of the closed channel for the grid-resolution test

Cases	Re_τ $= u_\tau\delta/\nu$	*Domain size* $L_x \times L_z$	*Grid number* $N_x \times N_y \times N_z$	*Grid spacing* h_x^+	h_y^+	h_z^+
(I)	590	$8\pi\delta \times 4\pi\delta$	$192 \times 65 \times 192$	77.2	$1.6 \sim 44.9$	38.6
(II)	590	$8\pi\delta \times 4\pi\delta$	$256 \times 65 \times 256$	57.9	$1.6 \sim 44.9$	29.0
(III)	590	$8\pi\delta \times 4\pi\delta$	$384 \times 65 \times 384$	38.6	$1.6 \sim 44.9$	19.3
(IV)	590	$8\pi\delta \times 4\pi\delta$	$512 \times 65 \times 512$	29.0	$1.6 \sim 44.9$	14.5
(V)	590	$8\pi\delta \times 4\pi\delta$	$512 \times 65 \times 384$	29.0	$1.6 \sim 44.9$	19.3
DNS(Del Álamo)	550	$8\pi\delta \times 4\pi\delta$	$1536 \times 257 \times 1536$	8.9	~ 6.7	4.5

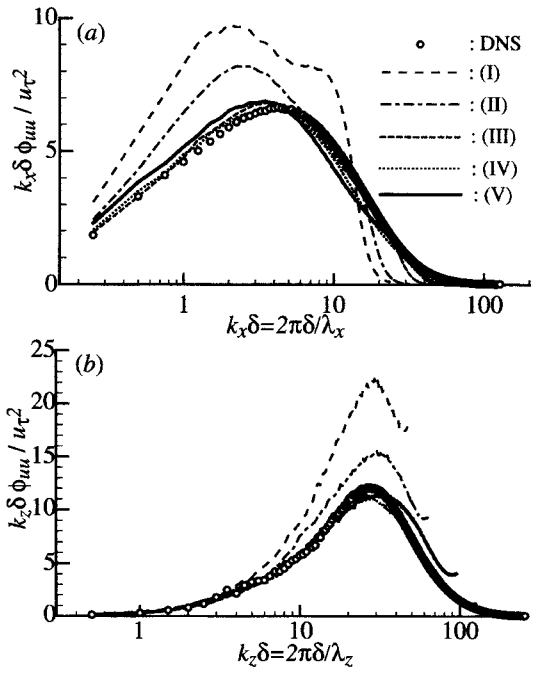

Figure 3: 1-D pre-multiplied power spectra of the streamwise velocity component at $y^+ \sim 15$: (a), streamwise; (b), spanwise.

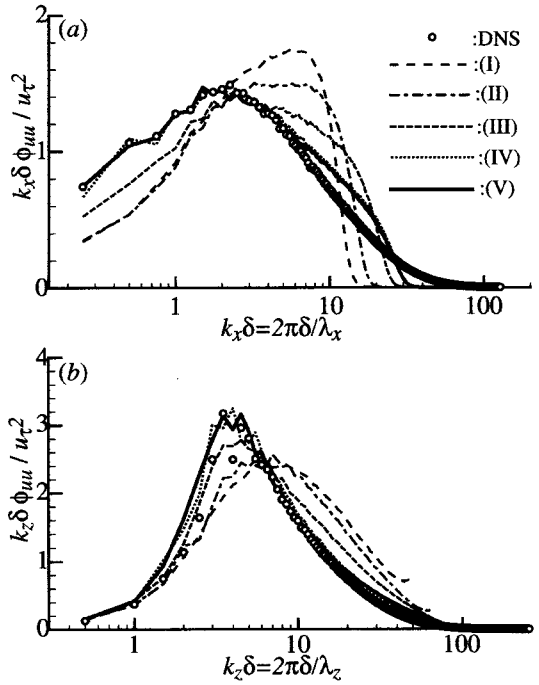

Figure 4: 1-D pre-multiplied power spectra of the streamwise velocity component at $y^+ \sim 280$:(a), streamwise; (b), spanwise.

the outer layer where large scales remarkably appear. The grid resolutions tested here are indicated as (I) to (V) in Table 4.

Figure 2 shows the GS turbulence statistics obtained by LES and DNS. As regards the mean velocity profiles, excellent agreement with DNS can be achieved in LES even in the case of the coarsest grid spacing. While rms of *grid scale* (GS) velocity shows slight dependence on the grid resolution especially in the near-wall region. The overestimation of the peak of the streamwise rms is worsen in the coarser grids, which contradict the theoretical expectation. This rather poor estimation of LES by using coarser grids has already been reported as one of the drawbacks of the dynamic Smagorinsky model(e.g. Tsubokura, 2001ab), and even the modified isotropic model adopted here cannot improve this tendency in coarser grid spacing.

On the other hand, we can see less dependence of the results on grid resolutions in the outer region ($y^+ > 100$)

and good correlation with DNS can be observed. But it does not necessarily mean that large scales in the outer region are well reproduced in all grid resolutions tested here.

The one dimensional pre-multiplied power spectra of the streamwise velocity component are shown in Figs. 3 and 4. We would like to note that the power spectrum multiplied by the wave number in the logarithmic plot indicates that the area under the profile is proportional to the power or energy included in the corresponding wave-number range.

In the near-wall region ($y^+ \sim 15$) where the streamwise rms shows maximum value, the pre-multiplied spectra obtained by DNS peak at $k_x\delta = 4.25$ and $k_z\delta = 27.5$ (*see* Fig. 3). These values are equivalent to $\lambda_x^+ \sim 810$ and $\lambda_z^+ \sim 130$ in the inner-scaling, which represents the size of the small-scale streaks (Kim et al., 1987). We can see that LES of coarser grids such as (I) and (II) completely fails to reproduce the spectral shape of DNS. It seems that the grid spacing of at least $\Delta_x^+ \sim 30$ and $\Delta_z^+ \sim 20$ corresponding to (V) are required to properly simulate the characteristics of the small scales near the wall.

In the middle of the outer layer ($y/\delta \sim 0.5$), DNS peaks at $k_x \sim 2.3$ and $k_z \sim 3.5, 4.5$, which amount to $\lambda_x \sim 2.8\delta$ and $\lambda_z \sim 1.8\delta, 1.4\delta$ in the outer scaling (*see* Fig. 4). We understand that these energetic modes at the lower wave number represent the characteristic size of the large scales. Contrary to the optimistic expectation that rather coarser grids of such as (I) and (II),which fail to capture the small scales near the wall, might be sufficient to reproduce the large scales in this region, Fig. 4 indicates that wavenumber of the spectral peak is larger estimated in (I) and (II). They also fail to reproduce the steep peak of DNS in the spanwise spectrum and only the moderate peak can be seen at the higher wavenumber. Estimating the grid resolution in the context of the reproduction of the peak of the spectra, we should adopt at least the grid resolution corresponding to (V) for the analysis of the large-scales.

SCALING

Neutral Cases

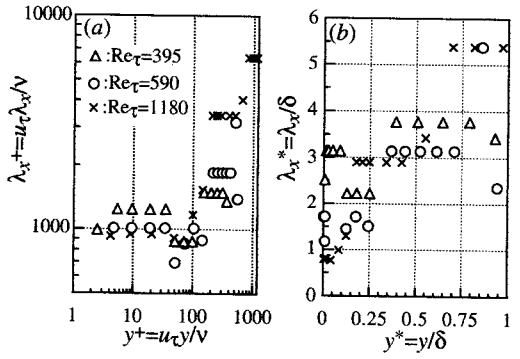

Figure 5: Streamwise peak wavelength of the pre-multiplied spectra at $Re_\tau = 395, 590, 1180$ in the neutral state:(a), inner-layer scaling; (b), outer-layer scaling.

The streamwise and spanwse wavelengths of the peak of the pre-multiplied power spectra of the streamwise velocity fluctuation at various Reynolds numbers are shown in Fig. 5 and 6 respectively. Data at three Reynolds numbers collapse well near the wall ($y^+ \leq 100$) in the inner-layer scaling(*see* Fig. 5(a) and 6(a)) and decaying asymptotically

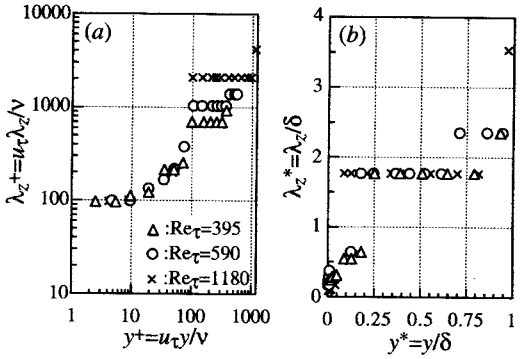

Figure 6: Spanwise peak wavelength of the pre-multiplied spectra at $Re_\tau = 395, 590, 1180$ in the neutral state:(a), inner-layer scaling; (b), outer-layer scaling.

to $\lambda_z^+ \sim 1000$ and 100 for streamwise and spanwise directions respectively. While in the region away from the wall ($y/\delta \geq 0.25$), the largest spanwise wavelength(*see* Fig. 6(b)) reaches approximately $\lambda_z \sim 1.8\delta$ independent of the Re_τ. The streamwise peak(*see* Fig. 5(b)) also shows the similar tendency and it reaches to $\lambda_x \sim 3\delta$ independent of the Re_τ. But contrarily to the spanwise peak, relatively larger scale of $\lambda_x \sim 5\delta$ is going to appear at the higher Reynolds number of 590 and 1180.

Stable Cases

The mean velocity profiles predicted by LES in the stable state are shown in Fig. 7. The typical feature of deviating from the logarithmic profile due to the stable stratification can be observed. It should be noted here that in the case at slightly larger than $Ri_\tau = 4.5 (Ri_\delta \sim 8.4 \times 10^{-2})$, flow cannot maintain turbulence state and become laminar.

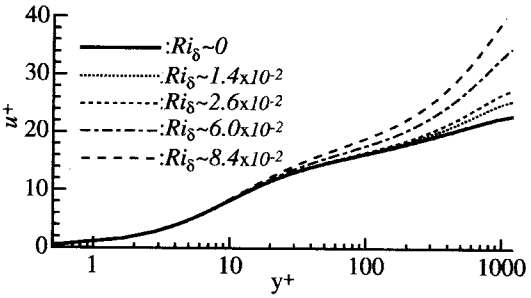

Figure 7: Mean velocity profiles at $Ri_\delta (\times 10^{-2}) \sim 0, 1.4, 2.6, 6.0, 8.4$ and $Re_\tau = 1180$.

The streamwise and spanwise wavelengths of the peak of the pre-multiplied power spectra of the streamwise velocity fluctuation at various Richardson numbers are shown in Fig. 8 and 9 respectively. We can see that the growth of the large-scales at or above the logarithmic-layer are strongly suppressed by the thermal stratification, and the streamwise and spanwise peak wavelengths of $\lambda_x \sim 3\delta$ and $\lambda_z \sim 2\delta$ above the logarithmic-layer in the neutral state are reduced to about δ and 0.5δ in the most stable condition tested here. It also should be noted that the height showing the maximum wavelength is shifted away from the wall due to the thermal stratification, say, from $y^+ \sim 100$(equivalent to $\sim 0.1\delta$) in the neutral state to about $y^+ \sim 500 (\sim 0.4\delta)$ at $Ri_\delta = 8.4 \times 10^{-2}$ for the spanwise wavelength(*see* Fig. 9).

In contrast to the large-scales, small structures near the wall are not affected strongly by the stable stratification and both the streamwise and spanwise peak wavelengths agree well at $y^+ < 50$, independent on the Richardson numbers tested here. Considering the fact that slightly stronger stratification than $Ri_\delta \sim 8.4 \times 10^2$ cannot maintain turbulence as mentioned at the beginning of this subsection, small-scale turbulence in the inner-layer is essential for turbulence production while the large-scales in the outer-layer seems to act on the production near the wall only secondarily even though they holds substantial energy as seen in Fig. 4(b).

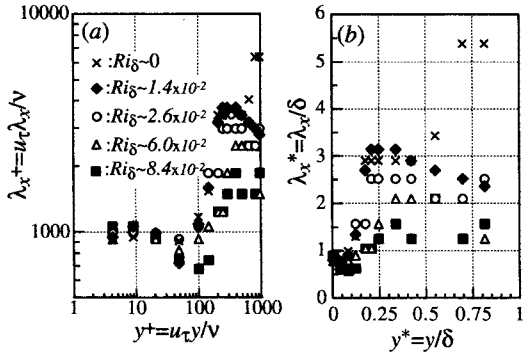

Figure 8: Streamwise peak wavelength of the pre-multiplied spectra at $Ri_\delta(\times 10^{-2}) \sim 0, 1.4, 2.6, 6.0, 8.4$ and $Re_\tau = 1180$:(a), inner-layer scaling; (b), outer-layer scaling.

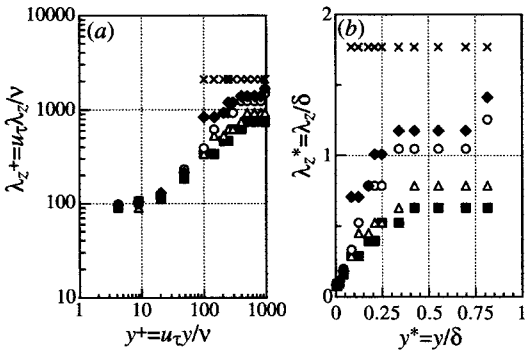

Figure 9: Spanwise peak wavelength of the pre-multiplied spectra at $Ri_\delta(\times 10^{-2}) \sim 0, 1.4, 2.6, 6.0, 8.4$ and $Re_\tau = 1180$:(a), inner-layer scaling; (b), outer-layer scaling.

CONCLUDING REMARKS

The findings of the present study can be summarised as follows:

1. Unexpectedly fine grid spacing of $h_x^+ \sim 30$ and $h_z^+ \sim 20$ for streamwise and spanwise directions is required to properly capture the 1-D pre-multiplied power spectrum and its peak at the lower wavenumber in the outer-layer where large-scales remarkably appear.

2. In the neutral state, the streamwise and spanwise peak wavelength of the pre-multiplied spectra collapse very well near the wall in the inner-scaling, while at or above the logarithmic-layer, their peak wavelength reach the maximum of $\lambda_x \sim 3\delta$ and $\lambda_z \sim 2\delta$ independent of the Reynolds number tested here.

3. In the stable state, the thermal stratification suppresses the growth of the peak wavelength at or above the logarithmic-layer for both streamwise and spanwise directions, contrary to the near-wall small structures being insensitive to the stable stratification tested here.

The first finding says that there seems to be a strong relation between the near-wall small-scales and the large-scales in the outer layer and may support the Townsend's attached eddy hypothesis and the subsequent physical models(e.g., Kim and Adrian in 1999), in which wall-turbulence is described as the evolutions of a hairpin structure attached on the wall and their subsequent packets.

REFERENCES

Del Álamo, J. C. and Jiménez, J., 2001, "Direct numerical simulation of the very large anisotropic scales in a turbulent channel", *Annual Research Briefs - 2001*, pp.329-341

Del Álamo, J. C. and Jiménez, J., 2003, "Spectra of the very large anisotropic scales in turbulent channels", *Phys Fluids*, **15**, to appear

DeGraaff, D. B., and Eaton, J. K., 2000, "Reynolds-number scaling of the flat-plate turbulent boundary layer", *J. Fluid Mech.*, **422**, pp.319-346

Germano, M., Piomelli, U., Moin, P., and Cabot, W. H., 1991, "A dynamic subgrid-scale eddy viscosity model", *Phys Fluids*, **A3**, pp.1760-1765

Ghosal, S., 1996, "An analysis of numerical errors in Large-Eddy Simulation of turbulence", *J. Comp. Phys.*, **125**, pp.187-206

Hunt, J. C. R. and Morrison, J., 2000, "Eddy structures in turbulent boundary layers", *Eur. J. Mech. B - Fluids*, **19**, pp.673-694

Jiménez, J., 1998, "The largest structures in turbulent wall flows", *Annual Research Briefs - 1998*, pp.943-945

Kawamura, H. and Abe, H., 2002, "DNS of turbulent scalar transport in a channel flow up to $Re_\tau = 640$ with $Pr = 0.025$ and 0.71", *Advances in Turbulence Research-2002*, pp.65-79

Kim, J., Moin, P. and Moser, R., 1987, "Turbulence statistics in fully developed channel flow at low Reynolds number", *J. Fluid Mech.*, pp.133-166

Kim, K. C. and Adrian, R. J., 1999, "Very large-scale motion in the outer layer", *Phys. Fluids*, **11**, pp.417-422

Lilly, D. K., 1992, "A proposed modification of the Germano subgrid-scale closure method", *Phys. Fluids*, **A4**, pp.633-635

Morinishi, Y., Lund, T. S., Vasilyev, O. V., and Moin, P., 1998, "Fully conservative higher order finite difference schemes for incompressible flow", *J. Comp. Phys.*, **142**, pp.1-35

Tsubokura, M., Kobayashi, T. and Taniguchi, N., 2001a, "Development of the isotropic eddy viscosity type SGS models for the dynamic procedure using finite difference method and its assessment on a plane turbulent channel flow", *JSME Int. J. Ser. B*, **44**, pp.487-496

Tsubokura, M., 2001b, "Proper representation of the subgrid-scale eddy viscosity for the dynamic procedure in large eddy simulation using finite difference method", *Phys. Fluids*, **13**, pp.500-504